Bioelectrochemistry 136 (2020) 107597

Contents lists available at ScienceDirect

Bioelectrochemistry

journal homepage: www.elsevier.com/locate/bioelechem

Reassessing the rationale behind herbicide biosensors: The case of a photosystem II/redox polymer-based bioelectrode

Panpan Wang [a], Fangyuan Zhao [a], Volker Hartmann [b], Marc M. Nowaczyk [b], Adrian Ruff [a,1], Wolfgang Schuhmann [a,*], Felipe Conzuelo [a,*]

[a] Analytical Chemistry - Center for Electrochemical Sciences (CES), Faculty of Chemistry and Biochemistry, Ruhr University Bochum, Universitätsstr. 150, D-44780 Bochum, Germany
[b] Plant Biochemistry, Faculty of Biology and Biotechnology, Ruhr University Bochum, Universitätsstr. 150, D-44780 Bochum, Germany

ARTICLE INFO

Article history:
Received 2 May 2020
Received in revised form 4 July 2020
Accepted 4 July 2020
Available online 6 July 2020

Keywords:
Photosystem II
Redox polymers
Biosensors
Inhibitors
Herbicides

ABSTRACT

Interfacing photosynthetic protein complexes with electrodes is frequently used for the identification of electron transfer mechanisms and the fabrication of biosensors. Binding of herbicide compounds to the terminal plastoquinone Q_B at photosystem II (PSII) causes disruption of electron flow that is associated with a diminished performance of the associated biodevice. Thus, the principle of electron transport inhibition at PSII can be used for herbicide detection and has inspired the fabrication of several biosensors for this purpose. However, the biosensor performance may reveal a more complex behavior than generally expected. As we present here for a photobioelectrode constituted by PSII embedded in a redox polymer matrix, the effect caused by inhibitors does not only impact the electron transfer from PSII but also the properties of the polymer film used for immobilization and electrical wiring of the protein complexes. Incorporation of phenolic inhibitors into the polymer film surprisingly translates into enhanced photocurrents and, in particular cases, in a higher stability of the overall electrode architecture. The achieved results stress the importance to evaluate first the possible influence of analytes of interest on the biosensor architecture as a whole and provide important insights for consideration in future design of bioelectrochemical devices.

1. Introduction

Photosystem II (PSII) is a fascinating photoactive protein complex that has captivated the attention of the scientific community as it is the only known naturally existing protein able to perform photochemical H_2O oxidation. PSII is the key element driving oxygenic photosynthesis, enabling the conversion of water, that is used as electron source for the process, into protons and molecular oxygen [1–5]. Light-induced charge separation and subsequent transfer of electrons and holes enables to accumulate the necessary oxidizing power to extract four electrons from two water molecules at the water oxidizing Mn_4CaO_5 cluster located at the electron donor side. On the opposite side of the protein complex, at the electron acceptor side, the primary plastoquinone electron-acceptor Q_A is reduced, subsequently passing two electrons in two consecutive photoreactions to the terminal plastoquinone Q_B. The reduced and protonated plastoquinol Q_BH_2 is then released enabling further electron transfer [6,7]. PSII does not stand only as a source of inspiration for the synthesis of novel (photo)catalysts providing the basis for an improved understanding about the intricate photoelectrochemical processes involved in the light-induced water oxidation reaction and transfer of high-energy electrons, but it also offers the possibility for integration within semi-artificial devices for different potential practical applications ranging from biophotovoltaic devices to the fabrication of biosensors [8,9]. As it has been shown, PSII protein complexes can be successfully interfaced with electrodes for this purpose and tremendous progress has been made to date involving photoelectrochemical investigations of PSII [4,10–14].

Several chemical compounds can interfere with the natural photosynthetic electron transport pathway by displacement of the Q_B plastoquinone from its binding site at the PSII protein complex and prevent the oxidation of the reduced primary electron-accepting plastoquinone Q_A by forward electron transfer, thus, hindering extraction of electrons from PSII [15,16]. This can be exploited for the detection of such inhibitor compounds commonly used as herbicides [17,18]. Thus, electrochemical herbicide biosensors have been reported either making use of isolated PSII

* Corresponding authors.
E-mail addresses: wolfgang.schuhmann@rub.de (W. Schuhmann), felipe.conzuelo@rub.de (F. Conzuelo).
[1] Present address: PPG Deutschland Business Support GmbH, PPG Packaging Coatings EMEA, Erlenbrunnenstr. 20, D-72411 Bodelshausen, Germany.

https://doi.org/10.1016/j.bioelechem.2020.107597
1567-5394/

[19–23], thylakoid membranes [24–28], or whole cells [29–33]. In all cases, the detection principle is based on the disrupted electron transfer at PSII caused by the inhibitor, which translates into an altered electrochemical response as a function of the herbicide concentration. Although the mentioned examples have shown the possibility for detection of different herbicides with an adequate sensitivity in terms of practical applications, the operation principle reveals to be rather complex, leading in certain cases to the incapability of detection of certain herbicide classes [20,24].

The possibility for an at least partial electron transfer bypassing the Q_B site has been reported for PSII immobilized on structured indium tin oxide-based electrodes, where a residual electron transfer to the electrode was observed in the presence of 3-(3,4-dichlorophenyl)-1,1-dimethylurea (DCMU) blocking the Q_B site [34,35]. This has been also shown for PSII in the presence of DCMU when using positively charged organometallic complexes in solution as exogenous electron acceptors [36,37]. Moreover, as we have recently shown in the evaluation of a PSII/redox polymer-based bioelectrode [38], partial photocurrents were still observed even in the presence of relatively large concentrations of DCMU in solution, indicating the possibility for electron extraction also when a redox polymer containing positively charged metal complexes as electron transfer mediator is used. As it has been shown for PSII [39,40], integration of enzymes into redox polymers makes an efficient electron transfer between the biomolecule and the electrode surface possible. The three-dimensional nature of the polymer layer allows for immobilization of a large amount of enzymes productively wired to the electrode surface via electron hopping through the polymer-bound redox moieties [41–43]. As a result, a significant increase of (photo)catalytic currents is obtained in comparison with the contribution from an enzyme monolayer immobilized on a given electrode surface.

However, in addition to the possible electron extraction from PSII at earlier stages in the electron transfer pathway, another important aspect, which was previously not considered, is the possible influence of the inhibitor species on the properties of the biosensor architecture, in particular when polymer matrices are used. In a solvated redox polymer, the hydrogel character of the polymer matrix enables permeation of water-soluble species with diffusion coefficients approaching those in water [44]. Since charge transport propagation relies on the oxidation/reduction of the redox centers tethered to the polymer backbone via a self-exchange process, simultaneous movement of counterions that compensate the charge is required to preserve electroneutrality [45]. Hence, the presence of different counterions may modify the redox polymer characteristics such as the degree of swelling and repulsion between electroactive sites, which has shown to affect the electron-hopping rate indirectly [46]. Moreover, the electrolyte composition may have an influence on the general electrochemical behaviour and activity of enzyme modified electrodes [47] and also on the response of enzyme/redox polymer films [48]. Although an important aspect, possible electrolyte effects and counterion effects are commonly overlooked in the characterization of enzyme/redox polymer films and should be considered in order to have a full picture about the electrochemical processes occurring at the assembly envisaged for biosensing applications.

Here, we present the evaluation of a PSII/redox polymer-based bioelectrode in the presence of herbicide compounds, where special attention is given to the effect caused by the inhibitor on the overall bioelectrode architecture. In contrast to the effect caused by DCMU, a phenylurea type herbicide, phenolic inhibitors similarly capable of blocking the Q_B site of PSII [49–52] have a drastic effect on the polymer matrix used for PSII immobilization and electrical wiring. Interestingly, a substantially more stable film is obtained, particularly when 2-*tert*-butyl-4,6-dinitrophenol (dinoterb) is incorporated into the polymer film. The effect caused by this nitrophenol compound is evaluated and discussed, demonstrating additional challenges for the development of corresponding biosensors and the need for a deeper understanding about effects caused by potential analytes of interest not only on the biorecognition element but also on all other components comprising the electrode architecture used for biosensor fabrication.

2. Materials and methods

2.1. Chemicals and materials

Tris-HCl (AppliChem); di-potassium hydrogen phosphate trihydrate, potassium dihydrogen phosphate, potassium chloride, methanol, and calcium chloride (VWR Chemicals); 2-(N-morpholino)ethanesulfonic acid (MES) and magnesium chloride (Carl Roth); poly(ethylene glycol)diglycidyl ether (PEGDGE, Mn = 400 g mol^{-1}, Polysciences); 2-*tert*-butyl-4,6-dinitrophenol (dinoterb), 3-(3,4-dichlorophenyl)-1,1-dimethylurea (DCMU), 2,4-dinitrophenol (DNP), 3,5-dibromo-4-hydrohybenzonitrile (bromoxynil), and bovine serum albumin (Sigma-Aldrich); citric acid monohydrate (J.T. Baker). All chemicals were of analytical grade and used without additional purification. The redox polymer poly(1-vinylimidazole-*co*-allylamine)-[Os(2,2′-bipyridine)$_2$Cl]Cl (P-Os) was synthesized and purified as described before [53]. The soluble Os-complex [Os-(1-(*n*-butyl)-imidazole)-(2,2′-bipyridine)$_2$Cl]PF_6 was synthesized as described elsewhere [54]. Photosystem II (PSII) was isolated from cultures of *Thermosynechococcus elongatus* as described in [39]. Photosystem I (PSI) from *T. elongatus* was obtained as previously reported [55]. All solutions were prepared using deionized water (ρ = 18 MΩ cm).

2.2. Electrode preparation

Prior to use, Au disk electrodes (2 mm diameter, CH Instruments) were polished using diamond suspensions (LECO) of decreasing particle sizes (0.3 μm, 0.1 μm, and 0.05 μm) and subsequently sonicated in ethanol and deionized water for 2 min. Afterwards, the electrodes were electrochemically cleaned by cyclic voltammetry in 0.5 M H_2SO_4 (15 cycles at 100 mV s^{-1} between −0.2 V and 1.6 V vs. Ag/AgCl/3 M KCl).

Stock solutions of inhibitors (30 mM) were prepared in methanol. For electrode modification, 2.5 μL of a mixture of P-Os (2.5 mg mL^{-1}), either PSI or PSII (1.0 mg mL^{-1}), PEGDGE (0.04 mg mL^{-1}), and inhibitor (if included, concentration in the mixture indicated) were drop-cast onto the electrode surface. Afterwards, the electrodes were incubated for 2 h in the dark at 4 °C.

2.3. Electrochemical measurements

Electrochemical measurements were performed using either a PalmSens2 (PalmSens) or a CHI 1030 (CH Instruments) potentiostat. A conventional three-electrode setup was used comprised of a Ag/AgCl/3 M KCl reference electrode, a Pt mesh as counter electrode, and the modified Au working electrode. Characterization of the PSII-based bioelectrodes was performed in 50 mM MES buffer pH 6.5, containing 10 mM $CaCl_2$, 10 mM $MgCl_2$, and 100 mM KCl, unless otherwise stated. Irradiation of the modified electrodes was performed using a Hg-Xe lamp (LC8 type 03, Hamamatsu Photonics) with red light (λ > 600 nm) by means of a lighting foil filter (#164, LEE Filters), with an effective light intensity reaching the sample surface measured to be 36 mW cm^{-2}. All measurements were performed at room temperature.

3. Results and discussion

In the development of bioelectrodes envisaged for sensing applications, it is of capital importance to evaluate and understand the influence of envisaged analytes on all elements involved in the electrode architecture. Therefore, it is not only important to consider the influence of analytes of interest on the recognition element but also on other additional components before performing an optimization of the bioassembly. Here, bioelectrodes constituted of PSII embedded in an Os-complex modified redox polymer (P-Os, see Fig. 1) used for immobilization and electrical wiring are investigated with respect to the influence of herbicide compounds on the redox polymer film. This was done by comparing the stability of the bioelectrode in the absence and presence of inhibitors belonging to two different structural families, i.e., urea and phenolic herbicides (Fig. 1).

In order to focus on the influence of herbicide compounds on the redox polymer film, evaluation of PSII/P-Os bioelectrodes that incorporate an inhibitor within the polymer film during electrode fabrication was performed. For this, a mixture of PSII, the redox polymer, a cross-linking agent, and the herbicide compound was used for electrode modification. The electrochemical characterization of electrodes fabricated in the presence and absence of DCMU revealed a decreased photocurrent response in the presence of the inhibitor (Fig. 2a). Nevertheless, a partial extraction of electrons from PSII was still observed, even when sufficient excess of DCMU was used to complex all immobilized PSII protein complexes.

Evaluation of the voltammetric Os^{2+}/Os^{3+} redox interconversion in the dark for the electrode incorporating DCMU within the film (Fig. 2b) showed a drastic decline in peak current after only few consecutive potentiodynamic cycles. This can be explained by the instability of the rather thin films used in this study. A lower loading with PSII used as biorecognition element was deliberately selected in comparison with previous reports [39], as it is essential for an improved sensitivity of potentially envisaged biosensors. The decreased electrochemical response over time was associated with a lower number of Os-centers in close proximity to the electrode surface due to an at least partial film detachment from the electrode surface. Note that during electrode preparation the protein complex/polymer film was cross-linked but not covalently attached to the Au electrode surface. In contrast, after incorporation of dinoterb, a nitrophenol inhibitor (see Fig. 1), within the film the recorded photocurrent was considerably larger than that for an electrode prepared in absence of inhibitor (Fig. 3a). Moreover, a considerably higher film stability was observed when comparing 100 consecutive potentiodynamic sweeps in the dark for electrodes prepared in the absence or presence of dinoterb in the film (Fig. 3b and c, respectively). A higher stability has been observed before for similar PSII-based bioelectrodes designed for energy conversion devices as a result of using higher PSII/P-Os loadings [39] and especially in combination with structured ITO as electrode substrates [40,56]. A progressive decay in the peak current was observed for the Os^{2+}/Os^{3+} redox interconversion at the thin-film PSII/P-Os electrode used in the present case (Fig. 3b). Instead, for the electrode incorporating dinoterb within the film, the decrease in peak current was slower (Fig. 3c) leading to a final peak current at the end of the experiment which was about three times larger than that for the PSII/P-Os electrode in absence of dinoterb.

In order to better understand the effect of dinoterb on the properties of the PSII/P-Os bioelectrode, a more detailed characterization was performed. First, the possibility of complexation of the nitrophenol compound with the polymer-bound Os-centers was evaluated (note that the chloro-ligand at the polymer bound Os-complex is only weakly coordinated and may be replaced by the phenolic compound via coordination of the —OH group to the metal center). For this, the soluble Os-complex [Os-(1-(*n*-butyl)-i

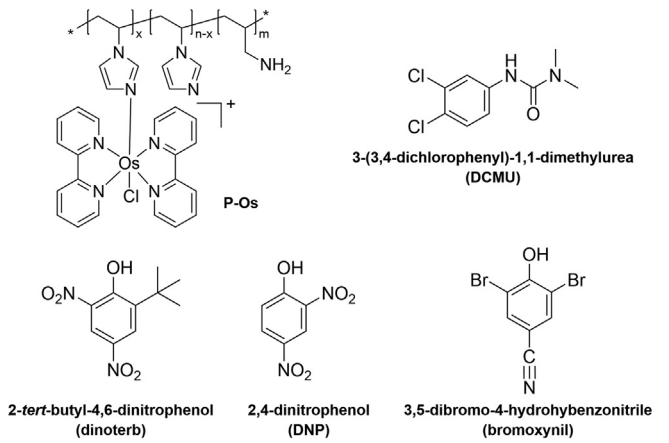

Fig. 1. Chemical structures of the redox polymer poly(1-vinylimidazole-*co*-allylamine)-[Os(2,2′-bipyridine)$_2$Cl]Cl (P-Os) and PSII inhibitor compounds used in this study.

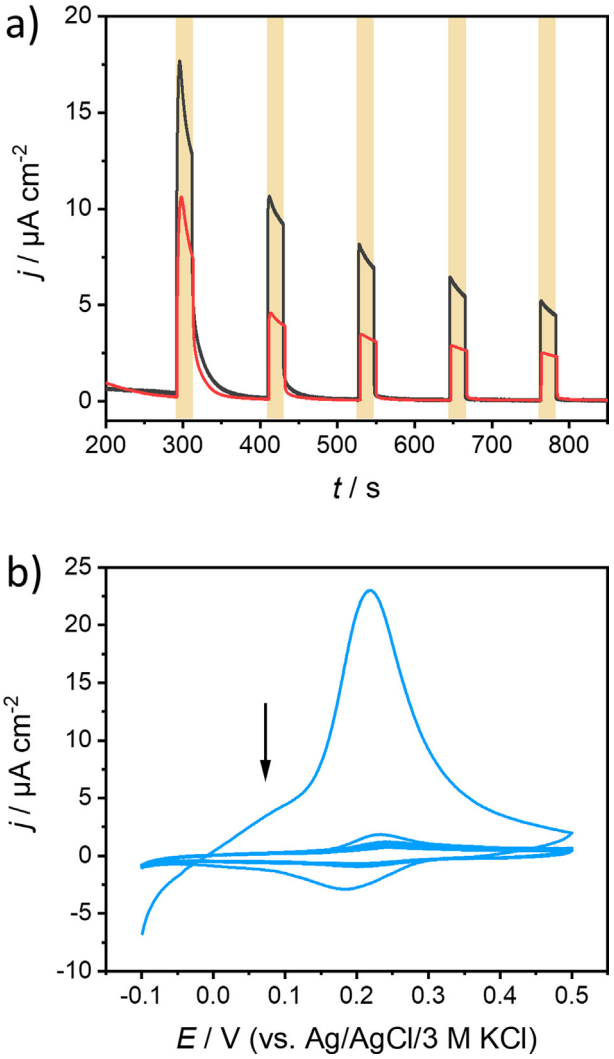

Fig. 2. (a) Chronoamperometric responses recorded with PSII/P-Os modified Au electrodes in the absence (gray curve) or presence (red curve) of 4.3 mM DCMU in the film. E_{app} = 350 mV vs. Ag/AgCl/3 M KCl. Irradiation with red light (yellow boxes, 36 mW cm^{-2}). (b) Cyclic voltammograms recorded for a freshly prepared electrode with 4.3 mM DCMU in the film (10 consecutive cycles, dark conditions). Scan rate: 5 mV s^{-1}. Electrolyte: 50 mM MES buffer, pH 6.5 (containing 10 mM $MgCl_2$, 10 mM $CaCl_2$, and 100 mM KCl). (For interpretation of the references to colour in this figure legend, the reader is referred to the web version of this article.)

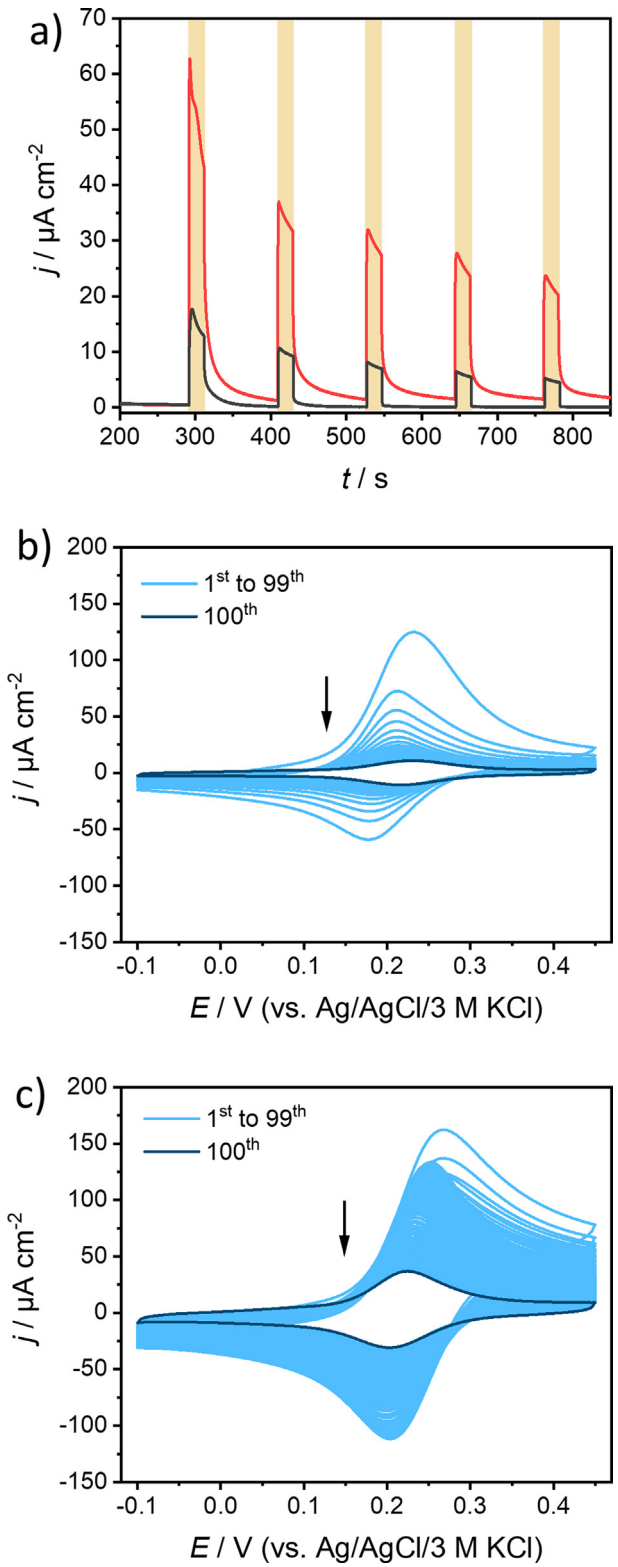

Fig. 3. (a) Chronoamperometric responses recorded with PSII/P-Os modified Au electrodes in the absence (gray curve) or presence (red curve) of 0.8 mM dinoterb in the film. E_{app} = 350 mV vs. Ag/AgCl/3 M KCl. Irradiation with red light (yellow boxes, 36 mW cm^{-2}). (b, c) Cyclic voltammograms recorded in the dark for freshly prepared electrodes in the absence (b) and presence (c) of 0.8 mM dinoterb in the film. 100 consecutive cycles, scan rate: 50 mV s^{-1}. Electrolyte: 50 mM MES buffer, pH 6.5 (containing 10 mM $MgCl_2$, 10 mM $CaCl_2$, and 100 mM KCl). (For interpretation of the references to colour in this figure legend, the reader is referred to the web version of this article.)

midazole)-(2,2′-bipyridine)$_2$Cl]$^+$ was synthesized and its electrochemical response in the absence and presence of dinoterb in solution was compared. The unchanged redox response measured in both cases indicated the absence of interactions between dinoterb and the Os-complex (Fig. S1). In addition, no electrochemical response was observed for dinoterb alone at the electrode surface within the potential range used (Fig. S2).

Subsequently, the influence of the dinoterb concentration in the mixture used for electrode modification was investigated. Electrodes fabricated in the same way but using different concentrations of dinoterb were electrochemically characterized by recording 100 consecutive potential cycles in the dark. The results revealed a clear influence of the inhibitor concentration on the film stability. A comparison of the last voltammogram recorded for the different electrodes (Fig. 4) showed increased peak currents with increasing concentrations of dinoterb until 3.3 mM, indicating higher film stability. At higher dinoterb concentrations a subsequent decrease in peak current was observed. Table S1 summarizes the peak current densities and peak separation for the different dinoterb concentrations in the film. Within the optimal range, the presence of dinoterb stabilized the film, making the structure more compact and stable as reflected by the larger Os^{2+}/Os^{3+} redox interconversion peak currents.

The film stability was also reflected in the photocurrent response. The photocurrent recorded with a PSII/P-Os modified electrode in a chopped light experiment at constant applied potential showed a fast and progressive current decay with time, reaching half of the initial photocurrent intensity after less than 5 min, corresponding to an effective illumination period of only 60 s (Fig. 5a). In contrast, the current recorded for the electrode prepared with 2.9 mM dinoterb in the film exhibited not only an initially higher photocurrent response, but also the photocurrent was stable for a longer time, reaching half of the highest photocurrent value after more than 35 min, i.e., 400 s of effective illumination (Fig. 5b). The initially observed raise in photocurrent was attributed to a gradual collapse of the film as a result of the time required for deprotonation of dinoterb short after placing the modified electrode into electrolyte solution. Therefore, the maximum photocurrent value (3rd illumination cycle) was considered as the initial time for estimating the stability of this bioelectrode. A summary of the half-lifetimes recorded with electrodes incorporating different concentrations of dinoterb in the film is presented in Fig. 5c. Moreover, under optimal conditions, in the presence of dinoterb substantially increased photocurrents of up to 70 µA cm^{-2} were observed (Fig. S3).

Replacing dinoterb in the film by 3,5-dibromo-4-hydrohybenzo nitrile (bromoxynil), another phenolic inhibitor (see Fig. 1), exhibited a similar initial effect on the photocurrent with large current densities measured upon irradiation (Fig. S4a–c), in comparison with films prepared in the absence of bromoxynil. However, a relatively fast decay in activity over time was observed. This was correlated with a lower stability of the PSII/P-Os layer on the electrode surface in comparison to the presence of dinoterb. After consecutive potential cycling in the dark for electrodes incorporating different amounts of bromoxynil, a substantial decrease in Os^{2+}/Os^{3+} peak currents was observed after 40 min of the experiment (Fig. S4d–f).

A plausible explanation for the observed stabilizing behavior caused by dinoterb within the PSII/redox polymer matrix is the possible influence of the deprotonated phenolic species on the polymer film. The phenolic inhibitors present rather low pK_a values: 4.80 for dinoterb [57], 4.20 for bromoxynil [58], and 4.09 for DNP [59]. Thus, they are fully deprotonated at the used conditions (pH 6.5), acting as additional counterions and affecting the

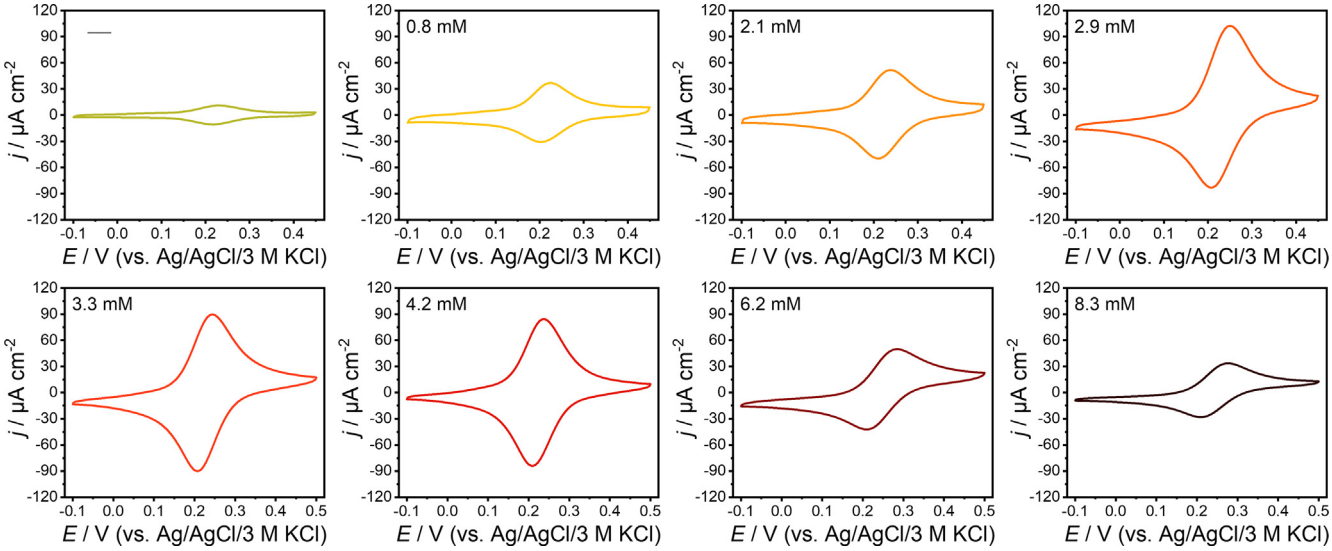

Fig. 4. Cyclic voltammograms recorded in the dark for PSII/P-Os modified Au electrodes in the absence or presence of dinoterb in the film (concentrations as indicated in the figure). The 100th cycle is presented for each case. Scan rate: 50 mV s^{-1}. Electrolyte: 50 mM MES buffer, pH 6.5 (containing 10 mM $MgCl_2$, 10 mM $CaCl_2$, and 100 mM KCl).

characteristics of the redox polymer such as the degree of swelling and repulsion between electroactive sites. In contrast, DCMU cannot act as a counterion due to the lack of a phenolic —OH function. As it has been already shown in earlier studies, the use of hydrophobic counterions favors hydrophobic interactions at redox polymer modified surfaces [44] and may cause a decrease in water content within the film as compared to hydrophilic anions, such as chloride [60,61]. Dinoterb, a dinitrophenol compound bearing the bulky and hydrophobic *tert*-butyl group, can influence the characteristics of the polymer film deposited on the electrode surface, providing an increase in film stability together with a possible collapse of the film in aqueous solutions. This will enhance the intimate contact between the enzyme and the redox mediator. Similar effects have been observed for PSI/P-Os bioelectrodes, where film collapse was forced by decreasing the number of positive charges within the polymer backbone at alkaline conditions leading to full deprotonation of imidazole units [54]. The presence of the rather bulky and non-polar *tert*-butyl group in *ortho*-position in dinoterb seems to be essential for the stabilizing effect, since this effect is drastically diminished in the case of bromoxynil, which only contains two bromide and one cyanide substituents at the aromatic core.

A control experiment was performed using 2,4-dinitrophenol (DNP) during film modification. DNP presents a similar chemical structure as dinoterb, only lacking the non-polar *tert*-butyl group (see Fig. 1). As expected, the substantial stabilizing effect observed before in the presence of dinoterb was not visible in this case and a progressive detachment of the polymer layer was observed (Fig. S5a,b), similarly to the results obtained in the presence of bromoxynil. The influence caused by dinoterb was exclusively related to the stability of the redox polymer film on the electrode surface but not due to a possible interaction with immobilized PSII as shown by replacing PSII in the film by an inactive protein, such as bovine serum albumin (BSA). As shown in Fig. S6, the stabilizing effect was also observed when dinoterb was incorporated into a BSA/P-Os film. Further evidence about the impact of dinoterb on film stability was obtained by investigating the film characteristics at different pH values. For this, photosystem I (PSI) was used instead of PSII for electrode fabrication. The use of PSI enabled to rule out any possible influence of the inhibitor, known to bind to the Q_B site of PSII, on the immobilized photosystem. At the same time, the use of PSI provided a more realistic comparison with the previously shown results due to the similar nature of both photosynthetic protein complexes. Two different sets of PSI/P-Os modified electrodes were prepared: a first set in the absence of inhibitor and a second incorporating dinoterb in the film. The individual electrodes were immersed in buffer solutions of different pH values and subjected to consecutive potentiodynamic cycling. The voltammetric response at the end of the experiment was analyzed.

The evaluation of PSI/P-Os modified electrodes showed an increase in peak current at pH values higher than 7.0 (Fig. 6a and c, Table S2). This was correlated with a $pK_a \approx 7$ for the conjugated acid of the imidazole groups of the polymer backbone. Deprotonation of the imidazolium cations leads to polymer film collapse at high pH values decreasing the distance between the polymer-bound redox centers, what is reflected in an enhanced electrochemical response [54]. On the other hand, for PSI/P-Os electrodes incorporating dinoterb in the film, an increased electrochemical response was observed already at pH $\geq$ 5.0 (Fig. 6b and c, Table S2). This observation was in agreement with the pK_a = 4.80 for dinoterb in aqueous solutions [57]. The results confirmed that deprotonated dinoterb acts as a bulky hydrophobic counterion and induces film collapse with a consequent stabilization of the redox polymer film deposited on the electrode surface.

4. Conclusions

The performance of PSII-based electrodes incorporating different inhibitor species within the redox polymer film was analyzed, showing that the possibility to extract electrons from the immobilized photosystem bypassing the terminal plastoquinone is common to several inhibitors known to block the Q_B binding site at PSII. Moreover, an *a priory* unexpected improved performance has been observed for bioelectrodes incorporating a phenolic inhibitor, i.e., dinoterb. A hypothesis for the observed effect associated with a higher stability of the polymer film deposited on the electrode surface has been proposed, related to the stabilizing effect of hydrophobic counterions, such as deprotonated dinoterb, leading to a collapse of the polymer film. The results highlight the importance to take into consideration the possible effect of additional counterions on redox polymer modified bioelectrodes. A

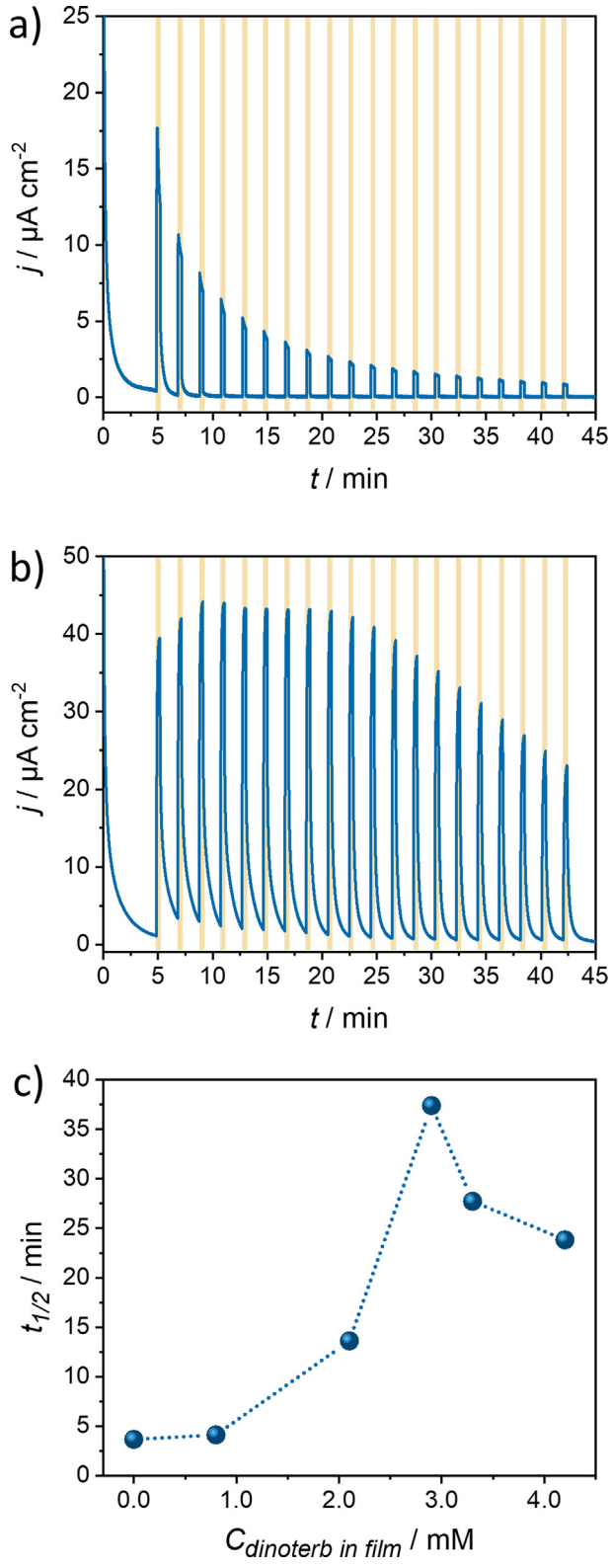

Fig. 5. Long-term evaluation of the photocurrent response recorded with modified Au electrodes: (a) PSII/P-Os, (b) PSII/P-Os in the presence of 2.9 mM dinoterb in the film, (c) summary of half lifetimes for the photocurrent obtained with electrodes prepared using different concentrations of dinoterb in the film. The dotted line is a guide for the eye only. E_{app} = 350 mV vs. Ag/AgCl/3 M KCl. Irradiation with red light (yellow boxes, 36 mW cm^{-2}). Electrolyte: 50 mM MES buffer, pH 6.5 (containing 10 mM $MgCl_2$, 10 mM $CaCl_2$, and 100 mM KCl). (For interpretation of the references to colour in this figure legend, the reader is referred to the web version of this article.)

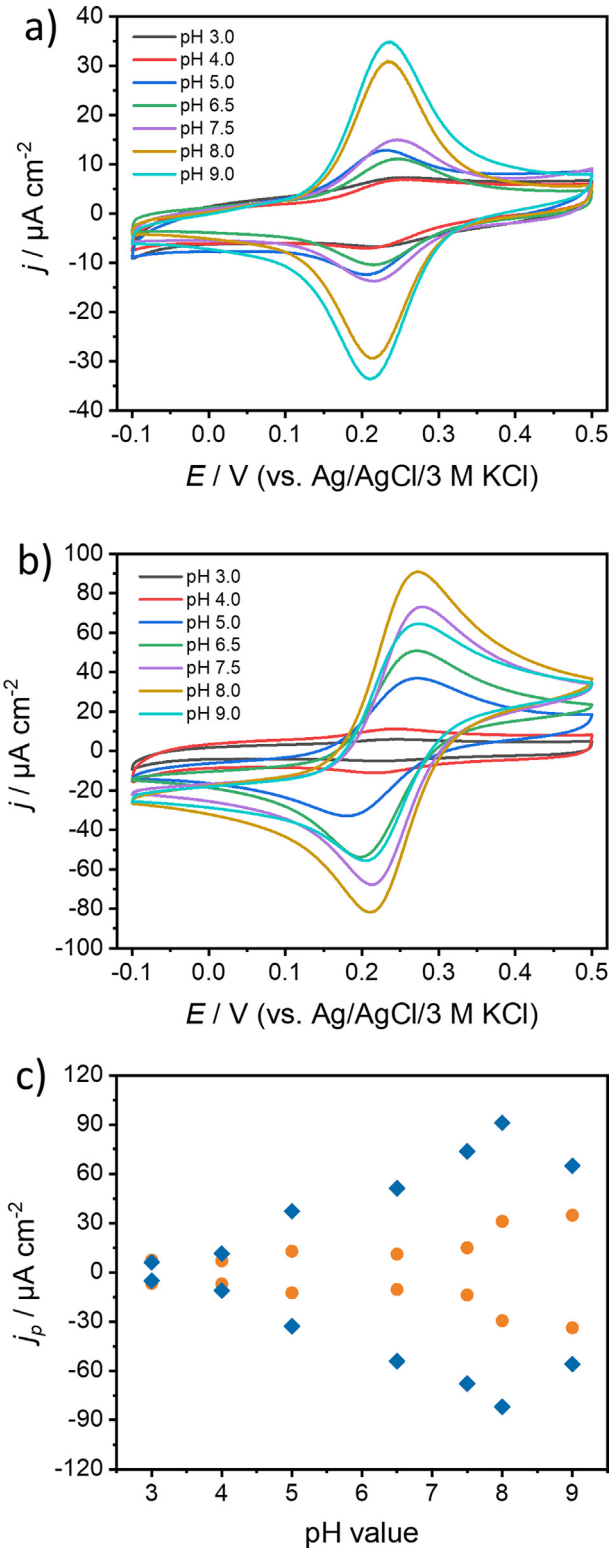

Fig. 6. Cyclic voltammograms recorded in the dark at different pH values. (a) PSI/P-Os modified Au electrodes. (b) PSI/P-Os modified Au electrodes in the presence of 3.3 mM dinoterb in the film. For each case, the last voltammogram after 100 consecutive cycles is presented. (c) Summary of anodic and cathodic peak current densities recorded at different pH values for electrodes fabricated in the absence (orange) and presence (blue) of dinoterb. Scan rate: 50 mV s^{-1}. Electrolyte: 50 mM phosphate-citrate or tris-HCl buffer (both containing 10 mM $MgCl_2$, 10 mM $CaCl_2$, and 100 mM KCl). (For interpretation of the references to colour in this figure legend, the reader is referred to the web version of this article.)

detailed understanding of the physicochemical and electrochemical processes involved is indispensable before the eventual fabrication and optimization of envisaged biosensing architectures.

Declaration of Competing Interest

The authors declare that they have no known competing financial interests or personal relationships that could have appeared to influence the work reported in this paper.

Acknowledgments

This work was supported by the Cluster of Excellence RESOLV (EXC 2033 – project number 390677874) funded by the Deutsche Forschungsgemeinschaft (DFG). P.W. is grateful for the financial support by the China Scholarship Council (CSC).

Appendix A. Supplementary material

Supplementary data to this article can be found online at https://doi.org/10.1016/j.bioelechem.2020.107597.

References

[1] J. Barber, Photosynthetic energy conversion: natural and artificial, Chem. Soc. Rev. 38 (2009) 185–196, https://doi.org/10.1039/b802262n.
[2] Y. Umena, K. Kawakami, J.-R. Shen, N. Kamiya, Crystal structure of oxygen-evolving photosystem II at a resolution of 1.9 Å, Nature 473 (2011) 55–60. https://doi.org/10.1038/nature09913.
[3] N. Cox, D.A. Pantazis, F. Neese, W. Lubitz, Biological water oxidation, Acc. Chem. Res. 46 (2013) 1588–1596, https://doi.org/10.1021/ar3003249.
[4] M. Kato, J.Z. Zhang, N. Paul, E. Reisner, Protein film photoelectrochemistry of the water oxidation enzyme photosystem II, Chem. Soc. Rev. 43 (2014) 6485–6497, https://doi.org/10.1039/c4cs00031e.
[5] W. Lubitz, M. Chrysina, N. Cox, Water oxidation in photosystem II, Photosyn. Res. 142 (2019) 105–125, https://doi.org/10.1007/s11120-019-00648-3.
[6] N. Nelson, A. Ben-Shem, The complex architecture of oxygenic photosynthesis, Nat. Rev. Mol. Cell Biol. 5 (2004) 971–982, https://doi.org/10.1038/nrm1525.
[7] N. Nelson, C.F. Yocum, Structure and function of photosystems I and II, Annu. Rev. Plant Biol. 57 (2006) 521–565, https://doi.org/10.1146/annurev.arplant.57.032905.105350.
[8] M.T. Giardi, E. Pace, Photosynthetic proteins for technological applications, Trends Biotechnol. 23 (2005) 257–263, https://doi.org/10.1016/j.tibtech.2005.03.003.
[9] B. Esper, A. Badura, M. Rögner, Photosynthesis as a power supply for (bio-) hydrogen production, Trends Plant Sci. 11 (2006) 543–549, https://doi.org/10.1016/j.tplants.2006.09.001.
[10] O. Yehezkeli, R. Tel-Vered, D. Michaeli, I. Willner, R. Nechushtai, Photosynthetic reaction center-functionalized electrodes for photo-bioelectrochemical cells, Photosyn. Res. 120 (2014) 71–85, https://doi.org/10.1007/s11120-013-9796-3.
[11] R. Tel-Vered, I. Willner, Photo-bioelectrochemical cells for energy conversion, sensing, and optoelectronic applications, ChemElectroChem 1 (2014) 1778–1797, https://doi.org/10.1002/celc.201402133.
[12] J.Z. Zhang, P. Bombelli, K.P. Sokol, A. Fantuzzi, A.W. Rutherford, C.J. Howe, E. Reisner, Photoelectrochemistry of photosystem II in vitro vs in vivo, J. Am. Chem. Soc. 140 (2018) 6–9, https://doi.org/10.1021/jacs.7b08563.
[13] N. Kornienko, J.Z. Zhang, K.P. Sokol, S. Lamaison, A. Fantuzzi, R. van Grondelle, A.W. Rutherford, E. Reisner, Oxygenic photoreactivity in photosystem II studied by rotating ring disk electrochemistry, J. Am. Chem. Soc. 140 (2018) 17923–17931, https://doi.org/10.1021/jacs.8b08784.
[14] J.Z. Zhang, E. Reisner, Advancing photosystem II photoelectrochemistry for semi-artificial photosynthesis, Nat. Rev. Chem. 4 (2020) 6–21, https://doi.org/10.1038/s41570-019-0149-4.
[15] W.F.J. Vermaas, G. Dohnt, G. Renger, Binding and release kinetics of inhibitors of $Q_{\bar{A}}$ oxidation in thylakoid membranes, Biochim. Biophys. Acta 765 (1984) 74–83, https://doi.org/10.1016/0005-2728(84)90159-2.
[16] A.W. Rutherford, A. Krieger-Liszkay, Herbicide-induced oxidative stress in photosystem II, Trends Biochem. Sci. 26 (2001) 648–653, https://doi.org/10.1016/S0968-0004(01)01953-3.
[17] M.T. Giardi, M. Koblízek, J. Masojídek, Photosystem II-based biosensors for the detection of pollutants, Biosens. Bioelectron (2001) 1027–1033, https://doi.org/10.1016/S0956-5663(01)00197-X.
[18] B. Bucur, F.-D. Munteanu, J.-L. Marty, A. Vasilescu, Advances in Enzyme-Based Biosensors for Pesticide Detection, Biosensors 8 (2018) 27, https://doi.org/10.3390/bios8020027.
[19] M. Koblizek, J. Masojidek, J. Komenda, T. Kucera, R. Pilloton, A.K. Mattoo, M.T. Giardi, A sensitive photosystem II-based biosensor for detection of a class of herbicides, Biotechnol. Bioeng. 60 (1998) 664–669.
[20] M. Koblízek, J. Malý, J. Masojídek, J. Komenda, T. Kucera, M.T. Giardi, A.K. Mattoo, R. Pilloton, A biosensor for the detection of triazine and phenylurea herbicides designed using photosystem II coupled to a screen-printed electrode, Biotechnol. Bioeng. 78 (2002) 110–116, https://doi.org/10.1002/bit.10190.
[21] J. Maly, J. Masojidek, A. Masci, M. Ilie, E. Cianci, V. Foglietti, W. Vastarella, R. Pilloton, Direct mediatorless electron transport between the monolayer of photosystem II and poly(mercapto-p-benzoquinone) modified gold electrode - new design of biosensor for herbicide detection, Biosens. Bioelectron. 21 (2005) 923–932, https://doi.org/10.1016/j.bios.2005.02.013.
[22] V. Bhalla, V. Zazubovich, Self-assembly and sensor response of photosynthetic reaction centers on screen-printed electrodes, Anal. Chim. Acta 707 (2011) 184–190, https://doi.org/10.1016/j.aca.2011.09.020.
[23] J. Masojídek, P. Souček, J. Máchová, J. Frolík, K. Klem, J. Malý, Detection of photosynthetic herbicides: algal growth inhibition test vs. electrochemical photosystem II biosensor, Ecotoxicol. Environ. Saf. 74 (2011) 117–122, https://doi.org/10.1016/j.ecoenv.2010.08.028.
[24] E. Touloupakis, L. Giannoudi, S.A. Piletsky, L. Guzzella, F. Pozzoni, M.T. Giardi, A multi-biosensor based on immobilized photosystem II on screen-printed electrodes for the detection of herbicides in river water, Biosens. Bioelectron. 20 (2005) 1984–1992, https://doi.org/10.1016/j.bios.2004.08.035.
[25] F. Bettazzi, S. Laschi, M. Mascini, One-shot screen-printed thylakoid membrane-based biosensor for the detection of photosynthetic inhibitors in discrete samples, Anal. Chim. Acta 589 (2007) 14–21, https://doi.org/10.1016/j.aca.2007.02.062.
[26] M. Rasmussen, S.D. Minteer, Self-powered herbicide biosensor utilizing thylakoid membranes, Anal. Methods 5 (2013) 1140, https://doi.org/10.1039/c3ay26488b.
[27] E. Touloupakis, C. Boutopoulos, K. Buonasera, I. Zergioti, M.T. Giardi, A photosynthetic biosensor with enhanced electron transfer generation realized by laser printing technology, Anal. Bioanal. Chem. 402 (2012) 3237–3244, https://doi.org/10.1007/s00216-012-5771-7.
[28] M. Rasmussen, A. Wingersky, S.D. Minteer, Comparative study of thylakoids from higher plants for solar energy conversion and herbicide detection, Electrochim. Acta 140 (2014) 304–308, https://doi.org/10.1016/j.electacta.2014.02.121.
[29] A. Avramescu, R. Rouillon, R. Carpentier, Potential for use of a cyanobacterium *Synechocystis sp.* immobilized in poly(vinylalcohol): Application to the detection of pollutants, Biotechnol. Tech. 13 (1999) 559–562, https://doi.org/10.1023/A: 1008991531206.
[30] A.I. Zamaleeva, I.R. Sharipova, R.V. Shamagsumova, A.N. Ivanov, G.A. Evtugyn, D.G. Ishmuchametova, R.F. Fakhrullin, A whole-cell amperometric herbicide biosensor based on magnetically functionalised microalgae and screen-printed electrodes, Anal. Methods 3 (2011) 509, https://doi.org/10.1039/c0ay00627k.
[31] I. Husu, G. Rodio, E. Touloupakis, M.D. Lambreva, K. Buonasera, S.C. Litescu, M. T. Giardi, G. Rea, Insights into photo-electrochemical sensing of herbicides driven by *Chlamydomonas reinhardtii* cells, Sensor. Actuat. B: Chem. 185 (2013) 321–330, https://doi.org/10.1016/j.snb.2013.05.013.
[32] M. Tucci, P. Bombelli, C.J. Howe, S. Vignolini, S. Bocchi, A. Schievano, A storable mediatorless electrochemical biosensor for herbicide detection, Microorganisms 7 (2019), https://doi.org/10.3390/microorganisms7120630.
[33] M. Tucci, M. Grattieri, A. Schievano, P. Cristiani, S.D. Minteer, Microbial amperometric biosensor for online herbicide detection: Photocurrent inhibition of *Anabaena variabilis*, Electrochim. Acta 302 (2019) 102–108, https://doi.org/10.1016/j.electacta.2019.02.007.
[34] M. Kato, T. Cardona, A.W. Rutherford, E. Reisner, Photoelectrochemical water oxidation with photosystem II integrated in a mesoporous indium-tin oxide electrode, J. Am. Chem. Soc. 134 (2012) 8332–8335, https://doi.org/10.1021/ja301488d.
[35] K. Brinkert, F. Le Formal, X. Li, J. Durrant, A.W. Rutherford, A. Fantuzzi, Photocurrents from photosystem II in a metal oxide hybrid system: Electron transfer pathways, Biochim. Biophys. Acta 2016 (1857) 1497–1505, https://doi.org/10.1016/j.bbabio.2016.03.004.
[36] G. Ulas, G.W. Brudvig, Redirecting electron transfer in photosystem II from water to redox-active metal complexes, J. Am. Chem. Soc. 133 (2011) 13260–13263, https://doi.org/10.1021/ja2049226.
[37] S. Khan, J.S. Sun, G.W. Brudvig, Cation effects on the electron-acceptor side of photosystem II, J. Phys. Chem. B 119 (2015) 7722–7728, https://doi.org/10.1021/jp513035u.
[38] F. Zhao, V. Hartmann, A. Ruff, M.M. Nowaczyk, M. Rögner, W. Schuhmann, F. Conzuelo, Unravelling electron transfer processes at photosystem 2 embedded in an Os-complex modified redox polymer, Electrochim. Acta 290 (2018) 451–456, https://doi.org/10.1016/j.electacta.2018.09.093.
[39] A. Badura, D. Guschin, B. Esper, T. Kothe, S. Neugebauer, W. Schuhmann, M. Rögner, Photo-induced electron transfer between photosystem 2 via cross-linked redox hydrogels, Electroanalysis 20 (2008) 1043–1047, https://doi.org/10.1002/elan.200804191.
[40] K.P. Sokol, D. Mersch, V. Hartmann, J.Z. Zhang, M.M. Nowaczyk, M. Rögner, A. Ruff, W. Schuhmann, N. Plumeré, E. Reisner, Rational wiring of photosystem II to hierarchical indium tin oxide electrodes using redox polymers, Energy Environ. Sci. 9 (2016) 3698–3709, https://doi.org/10.1039/C6EE01363E.
[41] A. Badura, T. Kothe, W. Schuhmann, M. Rögner, Wiring photosynthetic enzymes to electrodes, Energy Environ. Sci. 4 (2011) 3263–3274, https://doi.org/10.1039/c1ee01285a.

[42] A. Ruff, Redox polymers in bioelectrochemistry: Common playgrounds and novel concepts, Curr. Opin. Electrochem. 5 (2017) 66–73, https://doi.org/10.1016/j.coelec.2017.06.007.
[43] M. Yuan, S.D. Minteer, Redox polymers in electrochemical systems: From methods of mediation to energy storage, Curr. Opin. Electrochem. 15 (2019) 1–6, https://doi.org/10.1016/j.coelec.2019.03.003.
[44] A. Aoki, A. Heller, Electron diffusion coefficients in hydrogels formed of cross-linked redox polymers, J. Phys. Chem. 97 (1993) 11014–11019, https://doi.org/10.1021/j100144a019.
[45] C.P. Andrieux, J.M. Saveant, Electroneutrality coupling of electron hopping between localized sites with electroinactive counterion displacement. 1. Potential-step plateau currents, J. Phys. Chem. 92 (1988) 6761–6767, https://doi.org/10.1021/j100334a053.
[46] M.F. Mathias, O. Haas, Effect of counterion type on charge transport at redox polymer-modified electrodes, J. Phys. Chem. 97 (1993) 9217–9225, https://doi.org/10.1021/j100138a025.
[47] C. Carucci, A. Salis, E. Magner, Electrolyte effects on enzyme electrochemistry, Curr. Opin. Electrochem. 5 (2017) 158–164, https://doi.org/10.1016/j.coelec.2017.08.011.
[48] A. Suzuki, S. Tsujimura, Hofmeister effects on the glucose oxidase hydrogel-modified electrode, Electrochim. Acta 201 (2016) 228–232, https://doi.org/10.1016/j.electacta.2016.03.116.
[49] U. Johanningmeier, E. Neumann, W. Oettmeier, Interaction of a phenolic inhibitor with photosystem II particles, J. Bioenerg. Biomembr. 15 (1983) 43–66, https://doi.org/10.1007/BF00743219.
[50] D.E. Moreland, Research on biochemistry of herbicides: An historical overview, Z. Naturforsch. C 48 (1993) 121–131, https://doi.org/10.1515/znc-1993-3-402.
[51] Y. Nakajima, S. Yoshida, T.-A. Ono, Differential effects of urea/triazine-type and phenol-type photosystem II inhibitors on inactivation of the electron transport and degradation of the D1 protein during photoinhibition, Plant Cell Physiol. 37 (1996) 673–680, https://doi.org/10.1093/oxfordjournals.pcp.a028997.
[52] O. Belbachir, M. Matringe, D. Chevallier, M. Tissut, Physiological actions of dinoterb, a phenol derivative, Pestic. Biochem. Phys. 14 (1980) 309–313, https://doi.org/10.1016/0048-3575(80)90039-5.
[53] F. Conzuelo, N. Marković, A. Ruff, W. Schuhmann, The open circuit voltage in biofuel cells: Nernstian shift in pseudocapacitive electrodes, Angew. Chem. Int. Ed. 57 (2018) 13681–13685, https://doi.org/10.1002/anie.201808450.
[54] T. Kothe, S. Pöller, F. Zhao, P. Fortgang, M. Rögner, W. Schuhmann, N. Plumeré, Engineered electron-transfer chain in photosystem 1 based photocathodes outperforms electron-transfer rates in natural photosynthesis, Chem. Eur. J. 20 (2014) 11029–11034, https://doi.org/10.1002/chem.201402585.
[55] H. Kuhl, J. Kruip, A. Seidler, A. Krieger-Liszkay, M. Bunker, D. Bald, A.J. Scheidig, M. Rogner, Towards structural determination of the water-splitting enzyme. Purification, crystallization, and preliminary crystallographic studies of photosystem II from a thermophilic cyanobacterium, J. Biol. Chem. 275 (2000) 20652–20659, https://doi.org/10.1074/jbc.M001321200.
[56] F. Zhao, T. Bobrowski, A. Ruff, V. Hartmann, M.M. Nowaczyk, M. Rögner, F. Conzuelo, W. Schuhmann, A light-driven Nernstian biosupercapacitor, Electrochim. Acta 306 (2019) 660–666, https://doi.org/10.1016/j.electacta.2019.03.168.
[57] B.I. Escher, R.P. Schwarzenbach, J.C. Westall, Evaluation of liposome–water partitioning of organic acids and bases. 1. Development of a sorption model, Environ. Sci. Technol. 34 (2000) 3954–3961, https://doi.org/10.1021/es0010709.
[58] A.J. Cessna, R. Grover, Spectrophotometric determination of dissociation constants of selected acidic herbicides, J. Agric. Food Chem. 26 (1978) 289–292, https://doi.org/10.1021/jf60215a024.
[59] H.V. Halban, G. Kortüm, Die Dissoziationskonstanten schwacher und mittelstarker Elektrolyte: I. Die Dissoziationskonstante des α- Dinitrophenols und der Geltungsbereich der Debye-Hückelschen Grenzformel, Z Phys. Chem. 170A (1934) 351, https://doi.org/10.1515/zpch-1934-17033.
[60] S.M. Oh, L.R. Faulkner, Luminescent and redox probes of structure and dynamics in quaternized poly(4-vinylpyridine) films on electrodes, J. Am. Chem. Soc. 111 (1989) 5613–5618, https://doi.org/10.1021/ja00197a017.
[61] S.M. Oh, L.R. Faulkner, Electron transport dynamics in partially quaternized poly(4-vinylpyridine) thin films containing ferri/ferrocyanide, J. Electroanal. Chem. Interfacial Electrochem. 269 (1989) 77–97, https://doi.org/10.1016/0022-0728(89)80105-6.